Web-based Supplementary Materials : Treatment monitoring of HIV infected patients based on mechanistic models.

Mélanie Prague[1,2,*], Daniel Commenges[1,2], Julia Drylewicz [3] and Rodolphe Thiébaut[1,2]

[1] Univ. Bordeaux, ISPED, Centre INSERM U897-Épidémiologie-Biostatistique, F-33000 Bordeaux, France

[2] INSERM, ISPED, Centre INSERM U897-Épidémiologie-Biostatistique, F-33000 Bordeaux, France

[3] Department of Immunology, University Medical Center Utrecht, The Netherlands

**email:* melanie.prague@isped.u-bordeaux2.fr

1. Web Appendix A: "Activated cell model"

A graphical representation of the "activated cell model" presented as a differential equation system in the main article is available in Figure 1. We distinguish two different equilibrium points. The

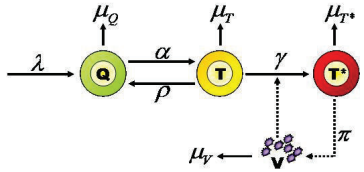

Figure 1. Graphical representation of the "activated cells model".

trivial equilibrium without infection is:

$$\begin{cases} Q_{0_-} = \frac{(\rho+\mu_T)\lambda}{\alpha\mu_T+\rho\mu_Q+\mu_Q\mu_T}, \\ T_{0_-} = \frac{\alpha\lambda}{\alpha\mu_T+\rho\mu_Q+\mu_Q\mu_T}, \\ T^*_{0_-} = 0, \\ V_{0_-} = 0. \end{cases} \quad (1)$$

If the basic reproductive number R_0 is higher than or equal to one, after the introduction of virions, the system stabilizes to a new non-trivial equilibrium:

$$\begin{cases} \bar{Q} = \frac{\lambda\gamma\pi+\rho\mu_{T^*}\mu_v}{\gamma\pi(\alpha+\mu_Q)}, \\ \bar{T} = \frac{\mu_{T^*}\mu_V}{\gamma\pi}, \\ \bar{T}^* = \frac{\lambda\gamma\pi\alpha-\rho\mu_V\mu_{T^*}\mu_Q-\alpha\mu_V\mu_{T^*}\mu_T-\mu_V\mu_{T^*}\mu_Q\mu_T}{\gamma\pi\mu_{T^*}(\alpha+\mu_Q)}, \\ \bar{V} = \frac{\lambda\gamma\pi\alpha-\rho\mu_V\mu_{T^*}\mu_Q-\alpha\mu_V\mu_{T^*}\mu_T-\mu_V\mu_{T^*}\mu_Q\mu_T}{\gamma\mu_{T^*}\mu_V(\alpha+\mu_Q)}. \end{cases}$$

Otherwise the trivial equilibrium (1) is asymptotically reached.

2. Web Appendix B: Proof of the convergence of $d^{t_k}_{opt}$ toward d_{crit} when Doob's consistency theorem applies

Let ξ be the random vector of biological parameters for a patient and ξ^* the true value of these parameters; here we omit the superscript i. We denote $P_\xi^{\mathcal{F}_{t_k}}$ the posterior law of ξ knowing the

available information $\mathcal{F}_{t_k}$ at time t_k. We also assume that we have identifiability (i.e., the information increases infinitely with time and the version of the posterior for ξ^* is essentially unique). With these assumptions, Doob's consistency theorem (see Van der (2000) p. 149 for details) ensures that the posterior distribution tends to a Dirac in the true value:

$$P_{\xi}^{\mathcal{F}_{t_k}} \xrightarrow[t_k \to \infty]{\mathcal{L}} \delta_{\xi^*}. \tag{2}$$

R_0 is a one-to-one function in the dose, thus, for a specific value of the biological parameters ξ, the critical dose is unique. Therefore, we can write the critical dose as a function of ξ implicitly defined as:

$$R_0 \left\{ \xi, d_{crit}(\xi) \right\} = 1. \tag{3}$$

Since the application $d_{crit}(\xi) : \mathbb{R}^p \mapsto \mathbb{R}$ is continuous, convergence in law of $d_{crit}(\xi)$ toward $d_{crit}(\xi^*)$ holds by composition. Since $d_{crit}(\xi^*)$ is a constant, convergence in law is here equivalent to convergence in probability, so we have : $d_{crit}(\xi) \xrightarrow[t_k \to \infty]{P} d_{crit}(\xi^*)$.

The properties of R_0 and (3) lead to a perfect match between the events $\{d_{crit}(\xi) < d\}$ and $\{R_0(\xi, d) < 1\}$. Thus we have:

$$\mathbb{P}\left[\left\{ d_{crit}(\xi) < d_{opt}^{t_k} \right\} | \mathcal{F}_{t_k} \right] \quad = \quad \mathbb{P}\left[\left\{ R_0(\xi, d_{opt}^{t_k}) < 1 \right\} | \mathcal{F}_{t_k} \right] = \omega, \tag{4}$$

This entails that $d_{opt}^{t_k}$ is the ω-quantile of $P_{d_{crit}(\xi)}^{\mathcal{F}_{t_k}}$. Since the law of $d_{crit}(\xi)$ tends to a Dirac in $d_{crit}(\xi^*)$ any quantile of the law tends to $d_{crit}(\xi^*)$:

$$d_{opt}^{t_k} \xrightarrow[t_k \to \infty]{P} d_{crit}(\xi^*).$$

3. Web Appendix C: Assessment of convergence reproducibility

We ran our optimization algorithm from 10 different starting points drawn at random at one standard deviation of the mean of the prior. The average coefficient of variation of the values at convergence is 0.3. In particular for $\tilde{\pi}$, $\tilde{\mu_V}$ and $\tilde{\mu_Q}$ we had only the order of magnitude. Thus the accuracy on the values of the parameters is not high. However we checked that the different

values obtained at convergence yielded essentially the same fit. We selected the patient with median viral load at the end of the study (labeled 663) and compared the fits (Figure 2) for three different stopping points: the one presented in Table 2 in the main article and stopping points with extreme values for the combination of parameters $\tilde{\pi}$, $\tilde{\mu_V}$ and $\tilde{\mu_Q}$ ($P_1 : (1.48, 0.65, -9.35)$ and $P_2 : (4.97, 4.18, -10.72)$). It is the case that these three sets of parameter values yield nearly the same trajectories for both viral load and CD4 count.

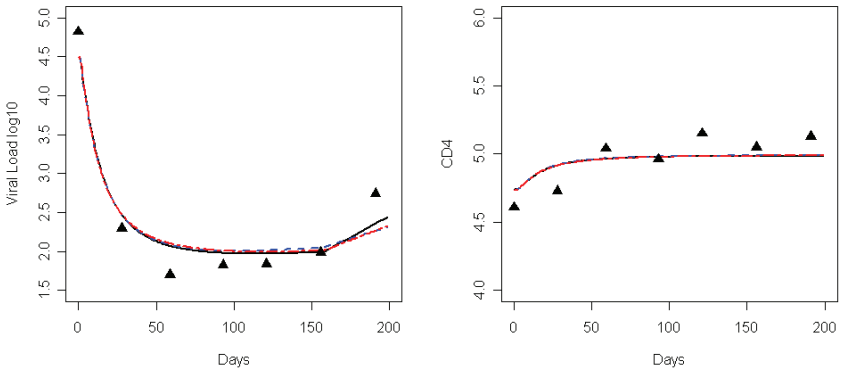

Figure 2. Viral load and total CD4 count fits for the patient with median viral load at the end of study for 3 different stopping points: the one presented in Table 2 in the main article (black plain line), P_1 (red point-dashed line) and P_2 (blue dashed line).

4. Web Appendix D: Predictive ability for treatment change (quartile patients)

We selected patients in the switch arm at each quartile values of the distribution of the viral load at the final visit (week 24) in the ALBI trial. The median patient (Q_2) is presented in the article. The patients for the other quartiles (Q_1 and Q_3) are presented Figures 3 and 4. The organization of the figures is the same as in the article. We present the viral load and the total CD4 count: this is a fit for the first treatment phase (d4t+ddI) and a prediction after the treatment switch to AZT+3TC.

We only used the first 12 weeks observations to update the parameters of the patients and predicted viral loads and CD4 counts after treatment switch. Most of the time, all the observations are in the 95% measurement error predictive interval for both viral load and CD4 count.

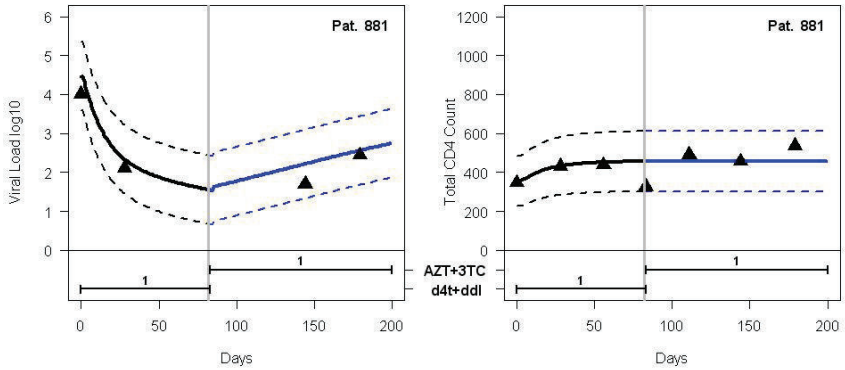

Figure 3. Prediction of patient 881 (Q_1) viral load and CD4 count after treatment change. We ignored a dose change from day 97 to day 99 because it only lasted 2 days and was considered as a reporting artefact.

5. Web Appendix E: Predictive ability for dose change (quartile patients)

We selected patients with dose changes at each quartile values of the distribution of the viral load at the final visit (week 24) in the ALBI trial. Patient 316 (at the 6^{th} deciles) is presented in the main article as an illustration because of a large range of behaviors. Nevertheless, this is not the one with the most reduced MSE compared to the ITT fit (without taking into account adherence) as it is shown Table 1.

The patients for the quartiles (Q_1,Q_2 and Q_3) are presented Figures 5 to 7. The organization of the figures is the same as in the article. We present the viral load and the total CD4 count: the fit

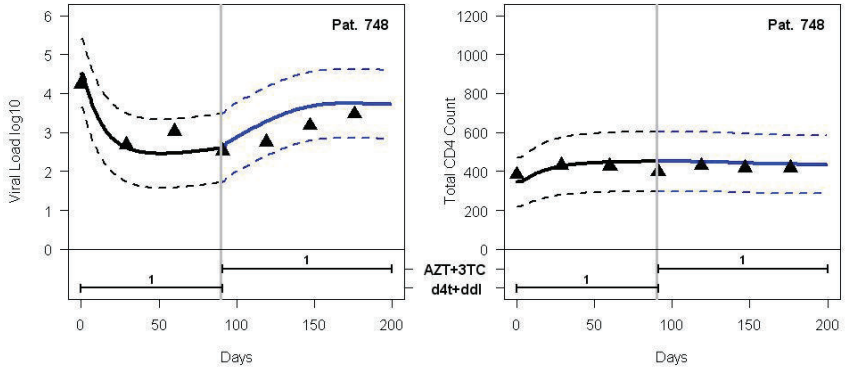

Figure 4. Prediction of patient 748 (Q_3) viral load and CD4 count after treatment change.

Table 1

Comparison of mean MSE between ITT model and our model accounting for dose changes.

	MSE for Viral Load		MSE for CD4 Count	
Patient	ITT	Dose model	ITT	Dose model
562 (Q_1)	0.18	0.15	2389	2163
660 (Q_2)	0.17	0.10	2364	476
316 (D_7)	1.25	0.15	4982	6062
664 (Q_3)	0.39	0.32	5354	5479

for the ITT analysis and the step by step predictions taking into account dose changes (parameters of the patient with random effects are updated each time we have an additional observation; this is labeled by a color change). Most of the time, all the observations are in the 95% measurement error predictive interval for both viral load and CD4 count. We expect a better prediction on viral load than on CD4 count.

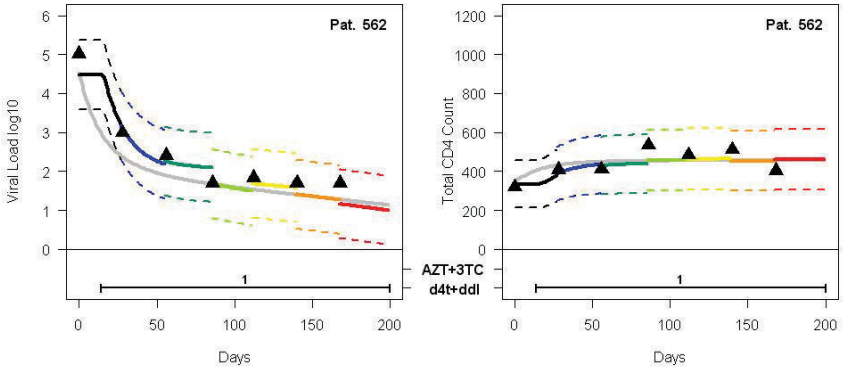

Figure 5. Prediction of patient 562 (Q_1) viral load and CD4 count accounting for dose changes.

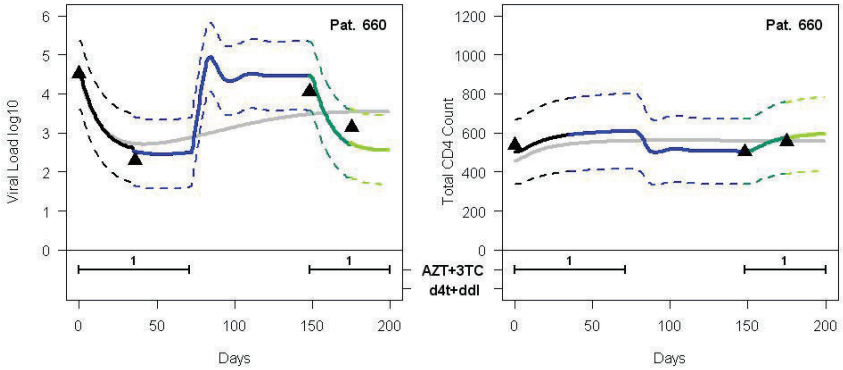

Figure 6. Prediction of patient 660 (Q_2 median) viral load and CD4 count accounting for dose changes.

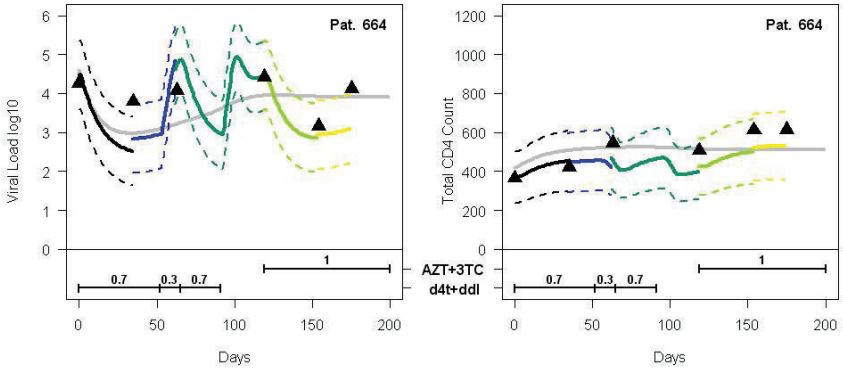

Figure 7. Prediction of patient 664 (Q_3) viral load and CD4 count accounting for dose changes.

References

Van der, A. (2000). *Asymptotic statistics*. Cambridge Series in Statistical and Probabilistic Mathematics, Cambridge University Press, UK.

Received September 2011. *Revised December* 2011.

Accepted January 2012.